





The Variation of the Solar Wind Correlation Scale and Taylor Scale Upstream of Mars Observed by MAVEN

Long Cheng^{1,2}  and Yuming Wang^{1,2,3} ¹ Deep Space Exploration Laboratory/School of Earth and Space Sciences, University of Science and Technology of China, Hefei 230026, People's Republic of China; chenglon@mail.ustc.edu.cn, ymwang@ustc.edu.cn² CAS Center for Excellence in Comparative Planetology/CAS Key Laboratory of Geospace Environment/Mengcheng National Geophysical Observatory, University of Science and Technology of China, Hefei 230026, People's Republic of China³ Collaborative Innovation Center of Astronautical Science and Technology, Hefei 230026, People's Republic of China

Received 2022 July 1; revised 2022 October 30; accepted 2022 November 6; published 2022 December 12

Abstract

The correlation scale and Taylor scale, which characterize the turbulence and dissipation levels, of the solar wind upstream of Mars are determined using the Mars atmosphere and volatile evolution magnetic field data from 2015 to 2020, which covers half of a solar cycle from the solar maximum to the solar minimum. Our analysis suggests that the correlation scale varies between 10 and 20 hr and the Taylor scale between 0.3 and 1 s. Applying the frozen-in flow approximation, we convert the two temporal scales to the two spatial scales, which are about $(1.5\text{--}3.0) \times 10^7$ km and 150–500 km, respectively. We further compare the correlation scale and Taylor scale to the sunspot number (SSN) to study the impacts of solar activity. The highest correlation coefficient between the correlation scale and the SSN is 0.78, where the two data sets are shifted by 16 months with the correlation scale behind the SSN. For the Taylor scale, the highest correlation coefficient is 0.52 with the time lag of 17 months. We also analyze the effective magnetic Reynolds number that is the square of the ratio of the two scales. It is more than 3×10^9 , suggesting the good assumption of the frozen-in flow. However, its correlation with the SSN is weak.

Unified Astronomy Thesaurus concepts: [Solar wind \(1534\)](#); [Mars \(1007\)](#); [Interplanetary magnetic fields \(824\)](#); [Solar activity \(1475\)](#); [Interplanetary turbulence \(830\)](#)

1. Introduction

Turbulences reside in the solar wind magnetic field with a broad range of scales, from the energy containing scale to the inertial range and the dissipation range (Tennekes & Lumley 1972; Goldstein et al. 1995; Tu & Marsch 1995; Verscharen & Wicks 2019). Typical scales are characterized to describe the properties of the solar wind turbulence. As shown in Figure 1 in Weygand et al. (2007), the correlation scale is the boundary between the energy containing scales and the inertial range (Smith et al. 2001). It represents the long wavelength end of turbulence in the inertial range, which is associated with the first break point of the power spectral density (Batchlor 1953; Weygand et al. 2006). From the aspect of data correlation, it represents the range that the magnetic field maintains correlation at a certain level and can be easily determined from the correlation function.

The Taylor scale (Taylor 1935) is a scale of the same order of magnitude as the Kolmogorov microscale, which is the boundary between the inertial range and the dissipation range (Kolmogorov 1991). The Kolmogorov scale is associated with the break point at the high frequency end of the inertial range, below which dissipative processes dominate (Denskat et al. 1983; Goldstein et al. 1995). Thus, the Taylor scale can also characterize the dissipative effects (Hinze 1975; Leamon et al. 1998). The Taylor scale can be measured relatively easily, it is associated with the curvature of the magnetic field at the origin and can be solved by the Taylor expansion (Weygand et al. 2007). Based on the correlation scale and Taylor scale, the effective magnetic Reynolds number can be further estimated

by calculating the square of the ratio of the correlation scale to the Taylor scale (Weygand et al. 2007).

In theory, the frozen-in flow approximation is needed for using the single-spacecraft data to measure the spatial properties of the solar wind, which indicates that the local Alfvén speed is much smaller than the solar wind speed, so the plasma is frozen in the solar wind flow (Taylor 1938). Since this approximation may not be valid over all the timescales, the better way to infer the spatial turbulence is using simultaneous two-point measurements (Matthaeus et al. 2005; Weygand et al. 2013). Nevertheless, the analysis based on single-point measurement is the only way for the earlier studies at 1 au and also the present studies beyond 1 au, since multispacecraft observations are rare.

The correlation scale and Taylor scale around 1 au have long been studied widely (Fisk & Sari 1973). Due to the lack of simultaneous measurements by multiple spacecraft, most of the earlier studies used single-point autocorrelation. Matthaeus et al. (2005) first use the simultaneous two-spacecraft measurements from the Wind, Advanced Composition Explorer (ACE), and Cluster to determine the correlation scale and the Taylor scale of $186 R_E$ and $0.39 R_E$, respectively. Weygand et al. (2007) employed Cluster data from different intervals in the magnetospheric plasma sheet for the first time and also the solar wind to determine the magnetic Taylor scale and the effective magnetic from multiple point measurements. Wicks et al. (2009) used simultaneous in situ observations by the ACE and Wind spacecraft to study the spatial correlation scale of the magnetic field and of the solar wind ion density for the first time. They found that there is a statistically significant increase in the correlation scale from the solar minimum to solar maximum. A similar result was found in the single-point analysis by Wicks et al. (2010). They conducted an



Original content from this work may be used under the terms of the [Creative Commons Attribution 4.0 licence](#). Any further distribution of this work must maintain attribution to the author(s) and the title of the work, journal citation and DOI.

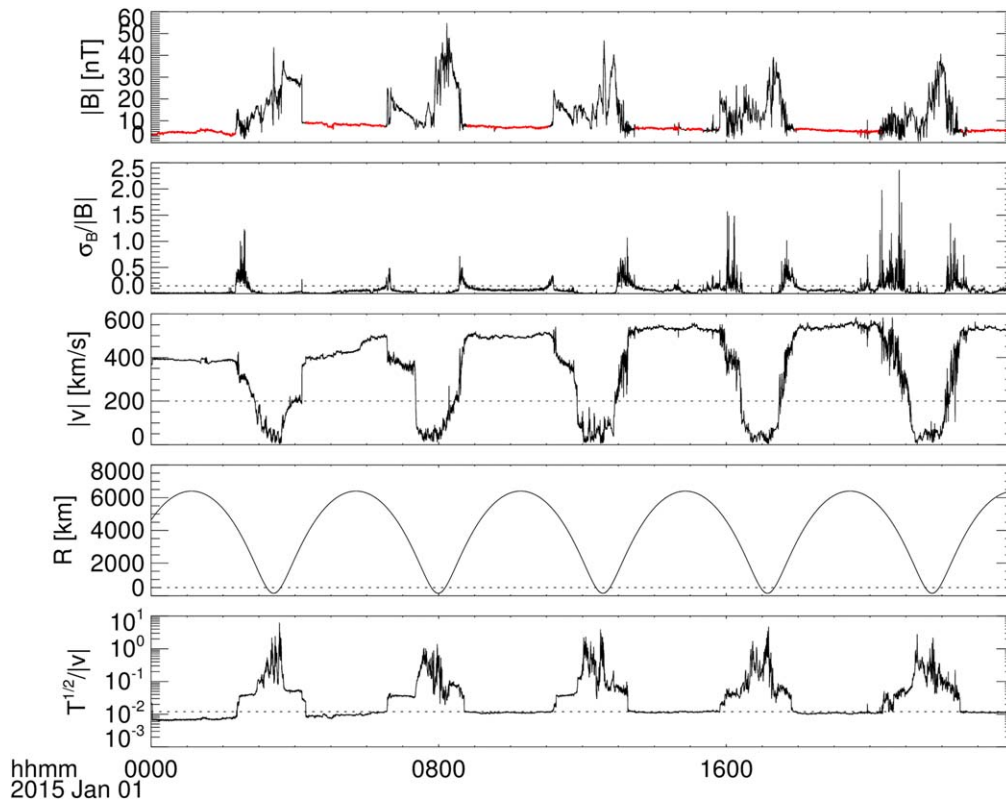


Figure 1. The magnetic field strength $|B|$, normalized magnetic field fluctuation levels $\sigma_B/|B|$, proton scalar temperature T , altitude R , and $\sqrt{T}/|v|$ computed from MAVEN MAG and SWIA data, where σ_B represents a root-sum-squared value of the 32 Hz fluctuation levels in all three components over a 4 s interval. The latter four parameters are used to select the undisturbed solar wind data. The selected upstream magnetic field data are shown with the red line.

autocorrelation study to determine the correlation scale of the magnetic field over two solar cycles at 1 au, and found that it increases by a factor of 2 from the solar minimum to solar maximum. They also found that the correlation scale is positively correlated with the solar wind quantity VB^2 that is the total magnetic energy passing in a given time, where V and B are the solar wind velocity and the magnetic field, respectively. This supports that the correlation scale is related to the energy containing scale of the solar wind (Wicks et al. 2010). Further, Zhou et al. (2020) have a detailed study on the effects of solar activity on the correlation scale and the Taylor scale. They used the data from 2001 to 2017, which covers an entire solar cycle, and showed the positive correlation between the scales and the sunspot number (SSN). The correlation coefficient between the correlation scale and the SSN is 0.56; the correlation coefficient for the Taylor scale and the effective magnetic Reynolds number is 0.92 and -0.82 , respectively.

The correlation scale of the magnetic field around Mars has also been studied. Marquette et al. (2018) used 35 months of solar wind data by the Mars atmosphere and volatile evolution (MAVEN; Jakosky et al. 2015) mission to conduct an autocorrelation analysis of the solar wind speed, density, dynamic pressure, and the interplanetary magnetic field (IMF). They found that the correlation scale of the IMF strength is about 20 hr. Franco et al. (2019) focused on the correlation scale of the ultra-low-frequency (ULF) waves around Mars. They used the Mars Express’s plasma data (Chicarro et al. 2004) during 2004–2015 and MAVEN plasma and magnetic field data during 2014–2016 to obtain the maps of the correlation scale of ULF waves around Mars. However, the correlation between the solar activity and the correlation

scale and Taylor scale of the IMF around Mars has not been revealed until now. In this study, we focus on effects of solar activity on the IMF scales upstream of Mars. In Section 2, we give a brief introduction to the data used in this work and criteria for selecting the upstream magnetic field data. In Section 3, we describe the method to determine the correlation scale and Taylor scale. In Section 4, we apply our method to obtain the variation of the scales and compare it to the SSN variation. The discussions and conclusions are provided in Section 5.

2. Data

For the measurements of solar wind magnetic field upstream of Mars, here we use the data from MAVEN’s magnetometer (MAG; Connerney et al. 2015). Since the end of 2014, MAVEN orbits Mars with the periapsis altitude of 150 km and the apoapsis altitude of 6200 km; it passes through the Martian magnetosphere and the upstream solar wind in cycles. In order to exclude the disturbed magnetic field downstream of the Martian bow shock, we need to select the upstream solar wind data first. Rather than identifying the upstream region by manually recognizing bow shocks of each orbits, we choose to select the upstream data automatically.

Here, we use the MAVEN in situ key parameters data bundle, which includes the plasma data from the Solar Wind Ion Analyzer (SWIA; Halekas et al. 2015) and the magnetic field data from MAG, with 8 s cadence above 500 km altitude, to identify the upstream regions. Following the method in Halekas et al. (2017), the criteria include $|v| > 200 \text{ km s}^{-1}$, $\sigma_B/|B| < 0.15$, $R > 500 \text{ km}$, $\sqrt{T}/|v| < 0.012$, where $|v|$ is the

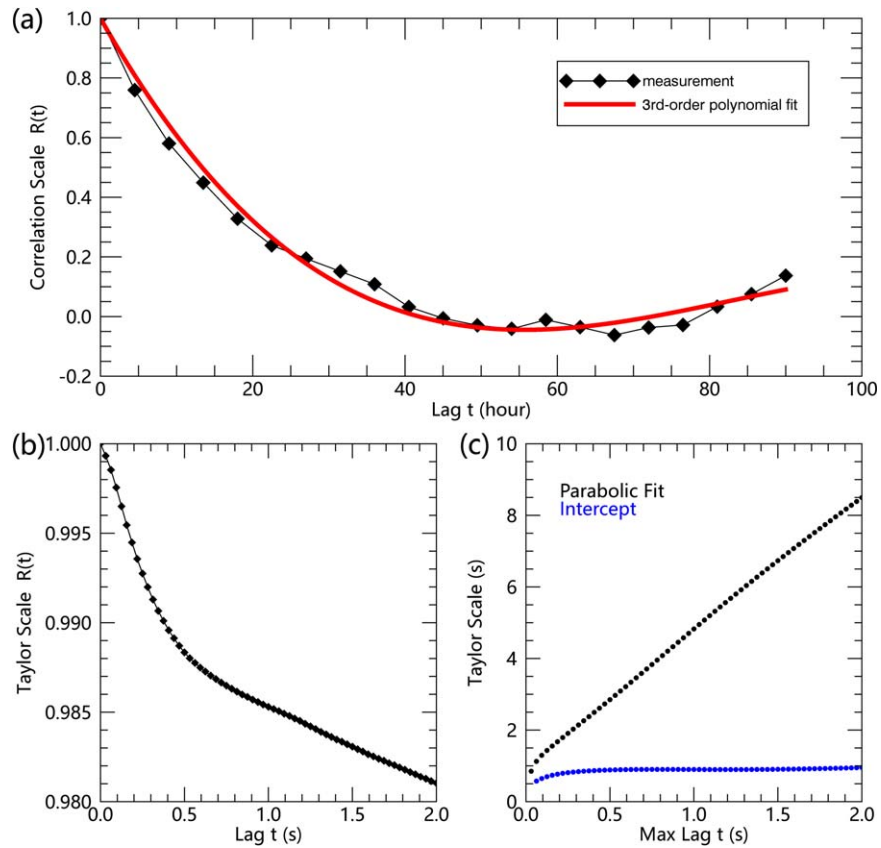


Figure 2. Magnetic field correlation function obtained from the single-spacecraft MAVEN measurement. Panel (a) shows the correlation function for the estimation of the correlation scale. The black line shows the measurements from the 8 s cadence data correlation coefficient and the red line shows the third-order polynomial fitting result. Panel (b) shows the correlation function for the estimation of the Taylor scale, measured from the 32 Hz magnetic field data. Panel (c) shows the result of the Richardson extrapolation method (see Weygand et al. 2007 in detail). The black line shows the increase in the value of the Taylor scales as the time shift becomes larger; the blue line shows the intercept value extrapolated from the linear fit to the Taylor scale points at different time shifts.

bulk flow speed, T is the proton scalar temperature, R is the altitude, $|\mathbf{B}|$ is the magnetic field strength, and σ_B is the fluctuation level of the magnetic field, provided by the key parameters data. These criteria were explained by Halekas et al. (2017) in detail.

Figure 1 shows an example of the application of this algorithm. Here we present the magnetic field data on 2015 January 1, and also the criteria of $|\mathbf{v}|$, $\sigma_B/|\mathbf{B}|$, R , $\sqrt{T}/|\mathbf{v}|$. The recognized upstream magnetic field is shown with the red line. It can be seen that the selected upstream data points are consistent with the bow shocks that are indicated by the magnetic field jumps.

3. Method

The correlation coefficient reflects how strong a relationship is between two variables. For the magnetic field data, it could be used to measure the relationship for two data sets measured at a different time or position with the same duration. If two-point measurements are available, we could have a correlation function that is related to the spatial separation. As for the single-spacecraft measurement here, the autocorrelation of the same data set is calculated, and the corresponding temporal separation can be converted to the spatial separation based on the frozen-in flow approximation. The correlation coefficient is unity at zero separation and decreases as the temporal or spatial separation becomes larger.

We first select a 3 month magnetic field data set with the 8 s cadence from MAVEN, and set all the data points downstream of the Martian bow shock to an invalid value. Then we choose another data set with a time shift, and select all the valid measurements in both original and shifted data sets, and calculate the Pearson correlation coefficient

$$r = \frac{\sum_{i=1}^N (x_i - \bar{x})(y_i - \bar{y})}{\sqrt{\sum_{i=1}^N (x_i - \bar{x})^2 \sum_{i=1}^N (y_i - \bar{y})^2}}. \quad (1)$$

By changing the time shift, we determine a correlation function of the time shift, $R(t)$, as shown in Figure 2(a). For the calculation of the correlation scale, we use a maximum time shift of 90 hr that is close to the value in Marquette et al. (2018), in which the correlation scale of the IMF is estimated to be about 20 hr. We use a time step of 4.5 hr, which is about MAVEN's orbital period, to avoid the sizable reduction of the valid upstream data points after time shifting (Marquette et al. 2018).

Usually, the correlation scale could be derived from the correlation function by fitting it with an exponential curve

$$R(t) = e^{-t/\lambda_c}, \quad (2)$$

where λ_c is the correlation scale. It means that when $t = \lambda_c$, the correlation coefficient between the magnetic field is reduced to be $1/e$; while the solar wind propagates over this scale, the magnetic field is uncorrelated. However, as illustrated in

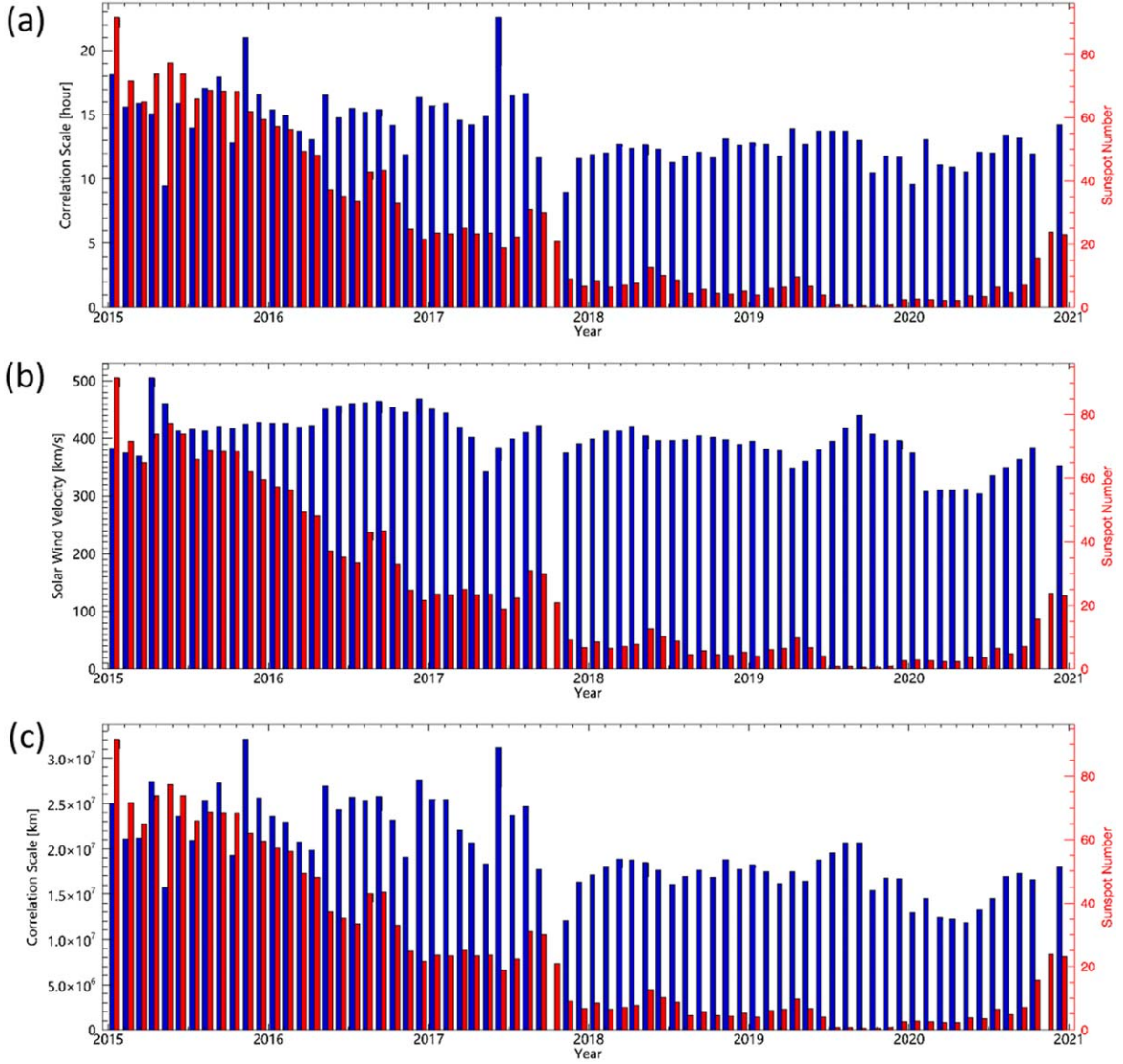


Figure 3. Variation of (a) temporal correlation scale, (b) solar wind flow speed, and (c) spatial correlation scale upstream of Mars. The spatial scale is the product of the temporal scale and the mean solar wind speed. The sunspot number is shown with the red line in each panel.

Marquette et al. (2018) and also in Figure 2(a), an exponential curve may not describe the correlation function properly, due to the data noise. Following the method in Borovsky (2012) and Marquette et al. (2018), here we use a third-order polynomial fitting instead, and still use the threshold of $1/e$ as the correlation scale.

The Taylor scale can also be derived from the correlation function, which is $\lambda_T = \sqrt{-R(0)/R''(0)}$ (Batchlor 1953; Matthaeus et al. 2005). Since $R(0) = 1$, λ_T is equivalent to the curvature of the correlation function at the origin. For small time shifts, the correlation function can be Taylor expanded as

$$R(t) = 1 - \frac{t^2}{2\lambda_T^2}. \quad (3)$$

To calculate $R(t)$ under small shifts, as shown in Figure 2(b), we use the 3 month data set of 32 Hz MAG data, and the time step is set to $1/32$ s with the maximum time shift of 2 s, which corresponds to the distance about 800 km for the solar wind propagation. Then we estimate the Taylor scale, λ_T , by fitting the obtained $R(t)$ with Equation (3). Here the Richardson

extrapolation technique is used (Weygand et al. 2007). Figure 2(c) shows an example of the result from the Richardson extrapolation. In the first step, we calculate the Taylor scales using the correlation function within different time shifts; the calculated Taylor scale increases as the shift is longer. In the second step, we extrapolate the values to the zero shift with a linear function; the intercept of the fitting line at the y-axis approached to be a stable value, which is determined as the Taylor scale at the origin, as the shift becomes longer (see Weygand et al. 2007 in detail).

While the correlation scale and Taylor scale are determined, we can further derive the effective magnetic Reynolds number

$$R_{\text{eff}} = \left(\frac{\lambda_c}{\lambda_T} \right)^2. \quad (4)$$

4. Results

The analyses of the MAVEN MAG data were performed from 2015 to 2020, which covers half of a solar cycle from the

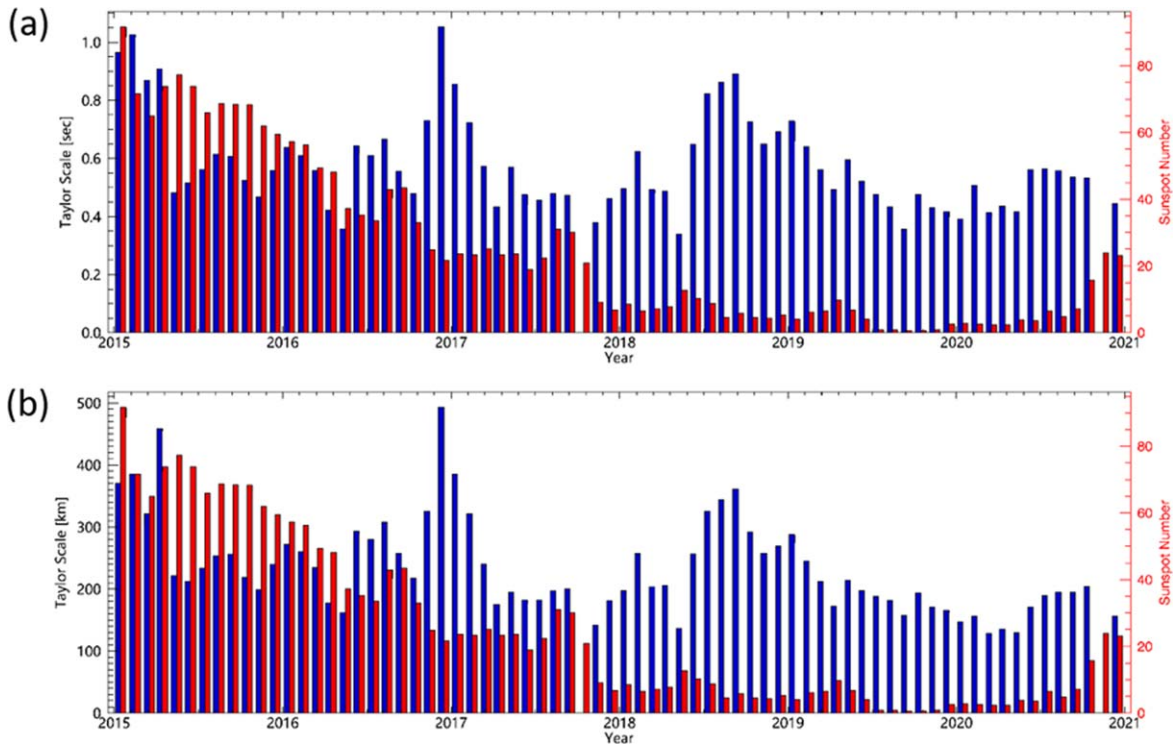


Figure 4. Similar to the Figure 3, but for variation of (a) temporal Taylor scale and (b) spatial Taylor scale upstream of Mars.

solar maximum to the solar minimum. We calculate the correlation scale and Taylor scale for each month, to investigate its correlation with the solar activity. The data set used for the analysis of each month includes 3 month data with the month of interest sitting at the center. For single-point measurements from MAVEN, the initial result is the temporal scale, then we multiply it with the mean solar wind speed during the period of the data set to obtain the spatial scale.

Figure 3(a) shows the result of the temporal correlation scale, which varies between 10 and 20 hr. During 2015–2017, the temporal correlation scale is about 15 hr, which is close to the result in Marquette et al. (2018). Since the mean solar wind speed around Mars fluctuates around 400 km s^{-1} (Figure 3(b)), we may estimate that the spatial correlation scale varies between 1.5 and $3.0 \times 10^7 \text{ km}$ (Figure 3(c)).

Figure 4 shows the result of the Taylor scale in temporal and spatial. In comparison to the correlation scale, the Taylor scales are more variable, which are from 0.3 to 1 s in temporal and from 150 to 500 km in spatial. The Taylor scale is comparable with the proton inertial length, 186 km, and the proton gyro-radius, 510 km, in the Martian upstream region, considering that the typical values of the upstream proton density, proton temperature, and the magnetic field are about 1.5 cm^{-3} , 100 eV, and 2 nT, respectively.

To analyze the modulation of solar activity on the correlation scale and Taylor scale upstream of Mars, we use the SSN data from the sunspot index and long-term solar observations database, calculate the mean SSN during the period of each 3 month data set, and superimpose it on Figures 3 and 4. In general, from 2015 to 2020, the solar activity was decreasing from decline phase to the minimum. The correlation scale and Taylor scale were also decreasing but were more variable rather than the SSN. The correlation coefficient between the correlation scale and the SSN is about 0.6, and that between the Taylor scale and the SSN is less than 0.4.

Considering that the variation of the IMF may lag behind the variation of the SSN, we calculate the correlation coefficients with different lags of the scales, relative to the SSN. As shown in Figure 5, the maximum correlation coefficient between the correlation scale and SSN is 0.78, while the lag between the correlation scale and SSN is 16 months. The maximum correlation coefficient between the Taylor scale and SSN is 0.52, with a lag time of 17 months. The variation of the solar wind speed also seems to be with a 16 month lag to the variation of the SSN.

Based on the correlation scale and Taylor scale, we can further calculate the effective magnetic Reynolds number, as shown in Figure 6. The effective magnetic Reynolds number is large and varies from 3×10^9 to 3×10^{10} , which indicates the good assumption of frozen-in IMF at 1.5 au. We find no relationship between the effective magnetic Reynolds number and the SSN in our study (see Figure 5(d)).

5. Discussions and Conclusions

In this study, we use the magnetic field from MAVEN during 2015–2020 to analyze the variation of the correlation scale and Taylor scale upstream of Mars. We first use the plasma data and magnetic field data to automatically select the undisturbed upstream data. Then we calculate the correlation function of each 3 month data set and fit it with a third-order polynomial curve. We determine the correlation scale by where the correlation function decays to $1/e$. Based on the Richardson extrapolation, we estimate the Taylor scale near the origin.

We focus on the relationship between the SSN and the correlation scale and Taylor scale. During the descent phase of the solar activity, both the correlation scale and the Taylor scale show a decreasing trend. The correlation coefficient between the correlation scale and the SSN is about 0.6, and that between the Taylor scale and the SSN is only about 0.4. However, if a

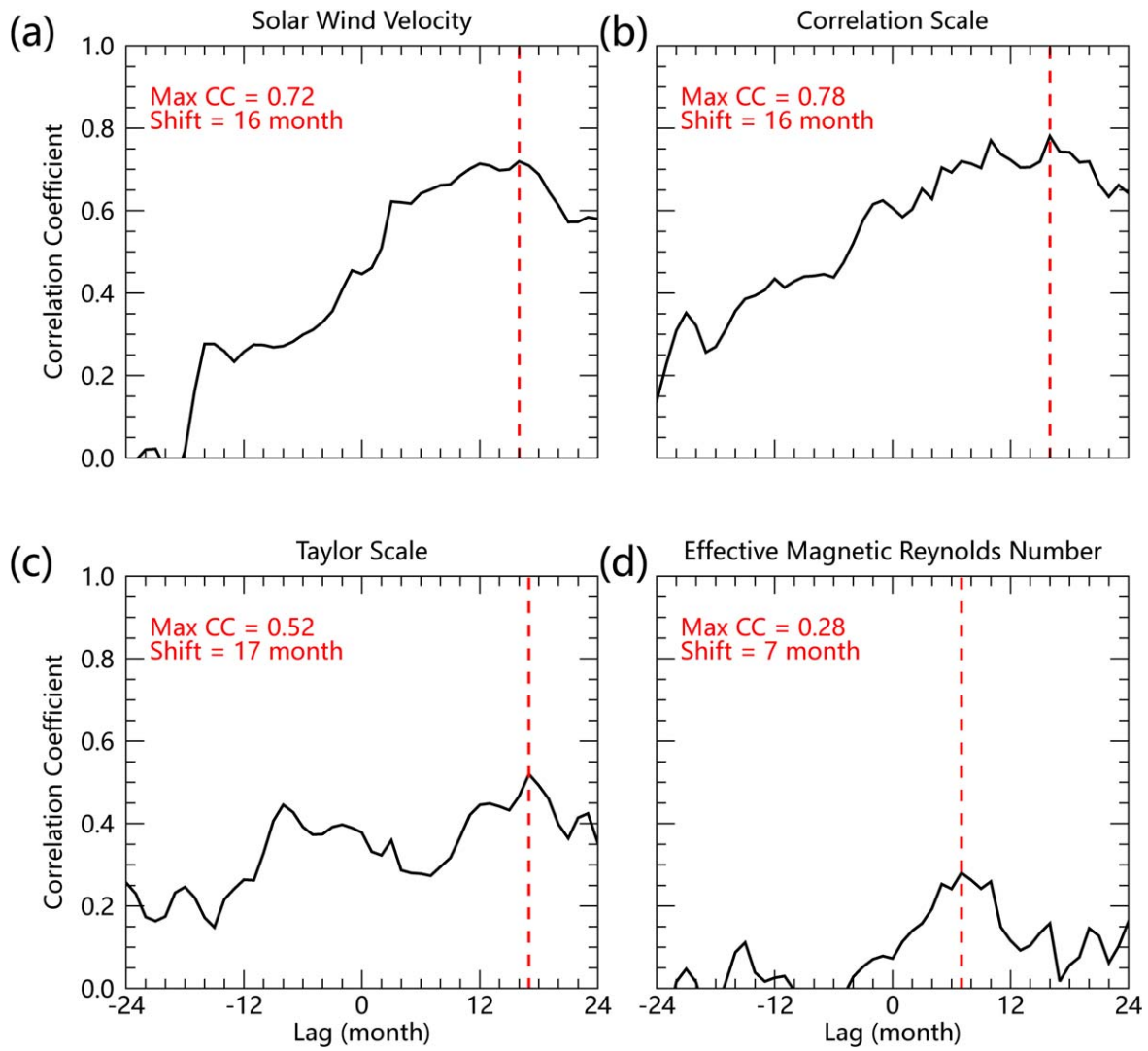


Figure 5. Correlation function between the sunspot number and (a) the solar wind velocity, (b) correlation scale, (c) Taylor scale, and (d) effective magnetic Reynolds number. The red lines denote where the maximum correlation is in the panel.

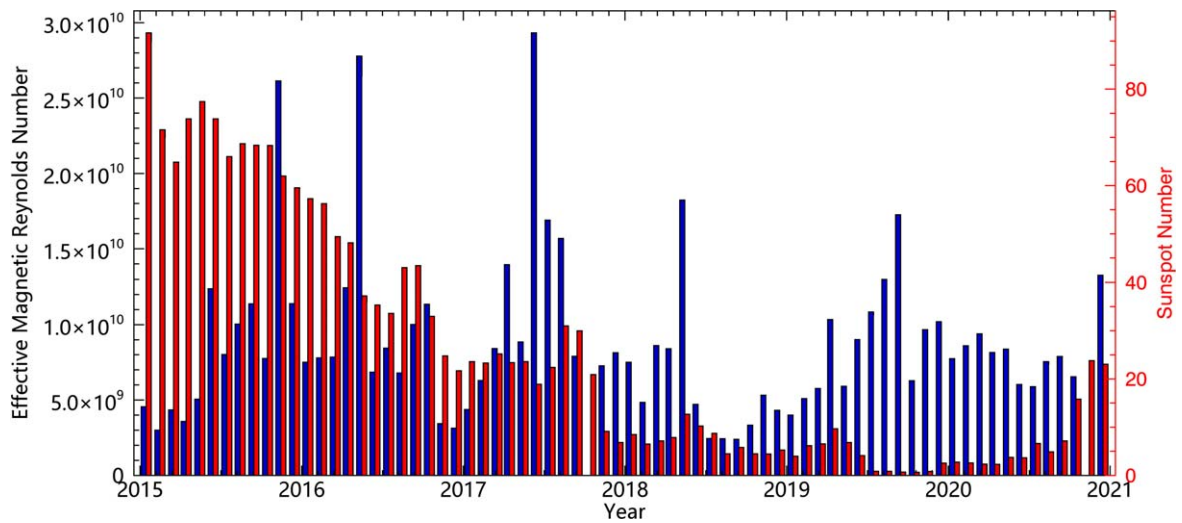


Figure 6. Variation of the effective magnetic Reynolds number derived from the correlation scale and Taylor scale. The sunspot numbers are also shown here.

time lag of 16 or 17 months is considered, the correlation coefficients between them increase to 0.78 and 0.52, respectively. The lag of the solar wind characteristics to the SSN for the best correlation may be attributed to the behavior of the open magnetic field on the Sun. As revealed by Wang et al. (2022), the variation of the area and flux of the solar open field lags behind the SSN's variation, which implicates the late opening of solar magnetic fields. They also found that the time delay is variable over solar cycles; since 2015, the variation of the open magnetic flux lags the SSN by about 1 to 2 yr (see Figure B1 in that paper for the details). Furthermore, the lags between the solar open fields and the SSN may rely on the solar cycle evolution below the solar surface and also the interior dynamo.

Compared with the studies at 1 au (Matthaeus et al. 2005; Weygand et al. 2007; Zhou et al. 2020), we find that the correlation scale at Mars is about 1 order higher than that at Earth, the Taylor scale at Mars is about 1 order lower, and therefore the effective magnetic Reynolds number is about 4 to 5 orders higher. We also find that the correlations between the scales and the SSN become weaker, and particularly the effective magnetic Reynolds number does not show a notable dependence on the SSN. It may be due to the further dissipation and expansion of the solar wind when it propagates from 1 to 1.5 au. At a farther distance, the solar wind expands into a larger space that may cause the correlation scale to increase, and the continuous dissipation of solar wind makes the magnetic energy and therefore the Taylor scale decrease. These changes probably reduce the imprint of the solar cycle variation, especially in terms of the magnetic Reynolds number. Alternatively, it may also be caused by the bias in the Taylor scale estimation using a single-spacecraft measurement. Bandyopadhyay et al. (2020) use the single and double-spacecraft data set from the Magnetospheric Multiscale Mission to estimate the Taylor scale, respectively; they found that, closer to the origin, the single-spacecraft estimate decays much more rapidly, which may be due to the time decorrelation with the solar wind turbulence in small scale. Meanwhile, they also found that, at large time shifts, the estimation of the correlation scale is consistent with previous reports based on single and multiple spacecraft data sets. It means that the single-spacecraft method would underestimate the Taylor scale and overestimate the effective magnetic Reynolds number. Hence, a more accurate estimation of the Taylor scale upstream of Mars may need double-spacecraft measurements. With the deployment of the magnetometer on board Tianwen-1's orbiter (Liu et al. 2020), there is one more spacecraft with a magnetometer orbiting Mars, apart from the MAVEN. In the future, we will seek the opportunity of simultaneous observations upstream of Mars between MAVEN and Tianwen-1's orbiter.

We thank the public data of MAVEN MAG and SWIA provided by NASA Planetary Data System. We acknowledge the sunspot number data from the WDC-SILSO, Royal Observatory of Belgium, Brussels (<https://www.sidc.be/silso/datafiles>). This research is supported by the Strategic Priority Program of CAS (XDB41000000) and the grants from NSFC (42130204 and 42188101). Y.W. is particularly grateful for the support of the Tencent Foundation.

ORCID iDs

Long Cheng  <https://orcid.org/0000-0003-0578-6244>

Yuming Wang  <https://orcid.org/0000-0002-8887-3919>

References

- Bandyopadhyay, R., Matthaeus, W. H., Chasapis, A., et al. 2020, *ApJ*, **899**, 63
- Batchlor, G. K. 1953, *The Theory of Homogeneous Turbulence* (Cambridge: Cambridge Univ. Press)
- Borovsky, J. E. 2012, *JGRA*, **117**, A05104
- Chicarro, A., Martin, P., & Trautner, R. 2004, in *ESA Special Publication 1240*, Mars Express: The Scientific Payload, ed. A. Wilson (Noordwijk: ESA), 3
- Connerney, J. E. P., Espley, J., Lawton, P., et al. 2015, *SSRv*, **195**, 257
- Denskat, K., Beinroth, H., & Neubauer, F. 1983, *JGeop*, **54**, 60
- Fisk, L. A., & Sari, J. W. 1973, *JGR*, **78**, 6729
- Franco, A. M. de S., Fränz, M., Echer, E., & Alves Bolzan, M. J. 2019, *E&PP*, **3**, 560
- Goldstein, M. L., Roberts, D. A., & Matthaeus, W. H. 1995, *ARA&A*, **33**, 283
- Halekas, J. S., Ruhunusiri, S., Harada, Y., et al. 2017, *JGRA*, **122**, 547
- Halekas, J. S., Taylor, E. R., Dalton, G., et al. 2015, *SSRv*, **195**, 125
- Hinze, J. O. 1975, *Turbulence* (New York: McGraw-Hill)
- Jakosky, B. M., Lin, R. P., Grebowsky, J. M., et al. 2015, *SSRv*, **195**, 3
- Kolmogorov, A. N. 1991, *RSPSA*, **434**, 9
- Leamon, R. J., Smith, C. W., Ness, N. F., Matthaeus, W. H., & Wong, H. K. 1998, *JGRA*, **103**, 4775
- Liu, K., Hao, X. J., Li, Y. R., et al. 2020, *E&PP*, **4**, 384
- Marquette, M. L., Lillis, R. J., Halekas, J. S., et al. 2018, *JGRA*, **123**, 2493
- Matthaeus, W. H., Dasso, S., Weygand, J. M., et al. 2005, *PhRvL*, **95**, 231101
- Smith, C. W., Matthaeus, W. H., Zank, G. P., et al. 2001, *JGRA*, **106**, 8253
- Taylor, G. I. 1935, *RSPSA*, **151**, 421
- Taylor, G. I. 1938, *RSPSA*, **164**, 476
- Tennekes, H., & Lumley, J. L. 1972, *A First Course in Turbulence* (Cambridge, MA: MIT Press)
- Tu, C. Y., & Marsch, E. 1995, *SSRv*, **73**, 1
- Verscharen, D., & Wicks, R. 2019, in 21st EGU General Assembly, 3114
- Wang, Y., Guo, J., Li, G., Roussos, E., & Zhao, J. 2022, *ApJ*, **928**, 157
- Weygand, J. M., Kivelson, M. G., Khurana, K. K., et al. 2006, *JGRA*, **111**, A11209
- Weygand, J. M., Matthaeus, W. H., Kivelson, M. G., & Dasso, S. 2013, *JGRA*, **118**, 3995
- Weygand, J. M., Matthaeus, W. H., Passo, S., Kivelson, M. G., & Walker, R. J. 2007, *JGRA*, **112**, A10201
- Wicks, R. T., Chapman, S. C., & Dendy, R. O. 2009, *ApJ*, **690**, 734
- Wicks, R. T., Owens, M. J., & Horbury, T. S. 2010, *SoPh*, **262**, 191
- Zhou, G., He, H.-Q., & Wan, W. 2020, *ApJL*, **899**, L32